A Practical Approach for internal energy tuning in LDI-MS: Porous Silicon substrates as a case study

Supplementary Material

Authors: Clara Whyte Ferreira[1 2 3], Bastien Cabrera-Tejera[2], Bernard Leyh[4], Romain Tuyaerts[1], Gilles Scheen[1], Yannick Coffinier[3†], Edwin De Pauw[2†], Gauthier Eppe[2†*]

1 Incize, 1348 Ottignies-Louvain-la-Neuve, Belgium
2 Mass Spectrometry Laboratory (MolSys Research Unit), University of Liège, 4000 Liège, Belgium
3 Univ. Lille, CNRS, UMR 8520 - IEMN, 59652 Villeneuve d'Ascq, France
4 Molecular Dynamics Laboratory (MolSys Research Unit), University of Liège, 4000 Liège, Belgium
† Equally contributed to the paper
*Corresponding author, e-mail: g.eppe@uliege.be

1. Density functional theory (DFT) computations results

The computations were performed using Gaussian 16, Revision B.01 and the base [B3LYP 6-311G++(d,p)]. For more accurate results, the calculation procedures was performed as follows:

i. Intact thermometer ions (parent) were submitted to a geometry optimization and frequency calculation routine
ii. The atoms corresponding to the neutral fragment (pyridine) were suppressed from the optimized parent geometry to obtain the charged fragment
iii. This charged fragment was then submitted to another geometry optimization routine
iv. The neutral fragment (pyridine) was also submitted to a geometry optimization routine

The dissociation energies (E_0) are obtained from:

$$E_0 = E_{charged\ fragment} + E_{neutral\ fragment} - E_{parent} \quad (1)$$

Computations were performed for the most commonly used thermometer ions. The results do not include the NO_2 para-substituted benzyl pyridinium salt because there is an inverse barrier on the fragmentation process, making it unsuitable for the effective temperature model proposed[1]. The detailed results are presented in Table 1 and Table 2.

Table 1 - Energy values (a.u. and eV) for substituted benzyl pyridinium salts, computed using Gaussian 16, Revision B.01, with the B3LYP 6-311G++(d,p) basis set.

	Energy (a.u.)				
BP salt substituent	Intact molecule (parent)	Charged fragment	Neutral fragment (pyridine)	E0 (a.u.)	E0 (eV)
mCH_3	-558.4869467	-310.0580391	-248.351255	0.077653	2.113033
$mOCH_3$	-633.7168772	-385.2849655	-248.351255	0.080657	2.19478
oCH_3	-558.4848417	-310.058726	-248.351255	0.074861	2.037063
pCH_3	-558.4875461	-310.0646426	-248.351255	0.071649	1.949656
pCN	-611.4125969	-362.972128	-248.351255	0.089214	2.427633
pCl	-978.776166	-730.3484943	-248.351255	0.076417	2.079402
pF	-618.4223224	-369.9933099	-248.351255	0.077757	2.115889

$pOCH_3$	-633.7179299	-385.3086308	-248.351255	0.058044	1.579459

Table 2 - Wave numbers for vibrational modes substituted benzyl pyridinium salts, computed using Gaussian 16, Revision B.01, with the B3LYP 6-311G++(d,p) basis set.

	BP salt substituent – Wave number (cm-1)							
Vibrational mode	mCH_3	$mOCH_3$	oCH_3	pCH_3	pCN	pCl	pF	$pOCH_3$
1	12.6098	14.3655	25.0902	8.9338	16.6082	12.4588	9.9084	13.2073
2	41.0095	33.1929	47.5931	40.1597	41.2378	45.6962	52.2895	42.6845
3	46.6856	61.9907	69.4552	55.1847	45.6651	51.1739	55.482	54.6698
4	69.8755	100.345	123.1838	55.9018	118.6125	141.8565	165.8159	104.6728
5	171.1303	170.9651	168.5747	159.8867	144.6183	176.885	183.3145	165.1979
6	213.2326	198.6699	184.8784	176.0512	191.2671	246.5554	274.5833	176.5097
7	236.7346	220.0633	268.2929	272.3354	261.3642	273.2944	300.8652	220.1051
8	272.3591	247.1129	294.1095	282.8247	282.4088	315.9224	347.5473	228.6276
9	293.2306	260.3746	311.5328	327.6806	333.1962	364.6161	404.0999	274.2495
10	394.5044	275.1825	404.8532	378.9046	402.213	403.706	424.6926	330.1615
11	404.3142	334.525	406.8578	404.1307	410.6729	419.053	426.2693	344.7616
12	439.3932	403.5388	447.7468	417.2056	423.8235	434.8014	446.5354	405.0067
13	447.7509	444.1682	451.2362	446.8326	445.5236	449.0725	509.7486	427.9004
14	508.5574	452.8267	501.6166	490.2141	481.5897	501.1481	521.3746	445.2539
15	527.5091	460.8111	530.8416	517.0787	561.9999	598.4512	610.2886	459.513
16	571.7859	540.8238	591.2206	612.0173	564.1421	646.2501	648.2829	523.7558
17	645.9414	562.7217	638.7506	653.9918	611.5123	656.3964	657.7591	543.0831
18	659.321	586.9133	659.2978	657.9078	656.6542	686.645	690.4005	612.4739
19	690.5326	659.2149	690.2175	691.0275	660.0254	692.057	720.0132	648.7106
20	712.753	661.5826	727.9908	720.0106	688.0837	737.0847	772.988	658.0182
21	756.6156	689.7974	757.4723	770.5945	718.5968	771.7596	787.0388	691.7178
22	773.3816	708.1846	768.7136	776.3435	757.671	789.9383	797.7968	724.1457
23	782.6121	763.3191	778.8238	782.8292	775.1959	839.5028	839.235	772.0558
24	822.8851	771.9243	809.8591	839.0666	803.7203	845.4877	860.6859	775.6775
25	881.1761	783.1787	864.1114	856.198	847.9123	865.7678	876.8598	787.5734
26	896.0924	811.6287	882.01	867.0303	857.5314	880.4874	880.916	830.5976
27	929.4397	879.9497	894.3658	881.503	875.2048	950.3813	950.2117	850.7851
28	943.5066	892.6107	950.2968	947.1436	878.5571	974.252	967.6286	867.535
29	960.1973	900.3562	975.7527	973.9365	952.4097	983.1215	983.3515	882.3969
30	984.5917	918.2185	983.9052	982.7915	979.2017	990.0005	986.5194	948.8048
31	1008.6506	962.1802	1005.841	994.0234	986.8295	1008.2516	1008.7293	961.817
32	1010.9307	983.5113	1009.2384	1009.3586	998.801	1032.3185	1029.7502	983.1089
33	1013.1018	993.6133	1019.5309	1016.583	1005.9402	1039.3447	1039.9232	984.464
34	1027.1444	1006.7499	1038.1973	1035.9683	1036.2251	1041.754	1041.595	1010.2816
35	1039.1046	1007.4817	1041.433	1039.7346	1038.8416	1075.6676	1075.6478	1022.1246
36	1041.7767	1037.7338	1059.7271	1041.4361	1042.1571	1109.426	1120.346	1039.3461
37	1063.9965	1041.8987	1072.6831	1062.0879	1075.5896	1120.8499	1128.9586	1039.956
38	1075.9797	1065.1178	1076.021	1075.8526	1121.5316	1131.9884	1130.4052	1041.9273
39	1118.1036	1076.1691	1120.7914	1120.051	1143.6172	1139.7809	1184.6362	1075.8035
40	1125.8342	1117.7102	1130.6046	1123.9501	1146.6667	1194.126	1194.0656	1114.8196

41	1130.9731	1121.5859	1141.483	1147.7493	1195.0613	1207.2152	1230.1983	1119.7149
42	1185.3071	1135.8162	1193.5072	1193.3321	1205.6048	1230.891	1236.5345	1143.2735
43	1193.7791	1167.3205	1194.8467	1210.103	1224.0727	1236.7539	1256.7729	1166.9083
44	1202.0895	1181.0301	1209.5061	1228.9757	1229.5858	1253.1886	1269.34	1192.8439
45	1233.3618	1193.7179	1231.4644	1232.9803	1234.9852	1298.7576	1297.3231	1198.0221
46	1254.6386	1199.0852	1237.2917	1242.5979	1245.3295	1322.3485	1326.5009	1202.1862
47	1270.1649	1214.2791	1259.9348	1258.2261	1307.1983	1351.3438	1357.1641	1230.5611
48	1297.2652	1233.9711	1300.4759	1293.4617	1327.0484	1375.8417	1376.592	1242.9783
49	1342.8068	1251.469	1322.2057	1337.0205	1356.4082	1399.6092	1399.7466	1257.7283
50	1350.9413	1299.0382	1348.7003	1357.434	1375.4204	1439.8447	1450.5242	1292.0654
51	1375.6477	1307.7777	1374.9498	1376.1661	1400.464	1488.8532	1489.7216	1303.8656
52	1398.5098	1334.4669	1398.7535	1397.994	1442.4383	1509.4407	1508.7252	1336.9302
53	1420.5623	1356.5073	1421.9205	1418.5476	1487.5932	1522.9317	1526.8605	1367.8706
54	1459.4453	1374.6877	1470.9883	1443.3774	1512.6815	1528.5994	1544.2602	1375.0883
55	1485.313	1398.9395	1487.6575	1488.7863	1527.9206	1606.4632	1617.1168	1395.9333
56	1488.3184	1471.19	1495.3479	1489.7893	1540.9742	1617.0525	1627.8108	1459.209
57	1501.2359	1484.3167	1500.3292	1491.5512	1600.1346	1632.6944	1643.9504	1477.6159
58	1509.5198	1489.8913	1509.9168	1507.773	1616.4109	1665.9969	1666.0835	1487.7988
59	1522.7542	1496.3473	1522.0223	1526.5595	1649.5172	3073.5449	3073.8817	1496.9875
60	1527.7688	1502.3885	1528.2465	1545.6711	1665.6111	3125.6029	3125.7114	1499.6435
61	1617.2537	1510.4127	1615.1457	1609.53	2345.8023	3165.3996	3168.2773	1506.7613
62	1624.7212	1523.1231	1617.4685	1617.7463	3076.1052	3166.7527	3169.3598	1526.0834
63	1642.8305	1528.7862	1642.9978	1648.0017	3128.1531	3199.589	3199.5912	1547.3425
64	1666.614	1617.0752	1666.1531	1666.6621	3168.0781	3206.8149	3208.0001	1605.5784
65	3034.2557	1620.3463	3019.469	3031.5921	3170.5167	3207.5619	3208.5007	1617.906
66	3072.6522	1643.6088	3063.976	3071.8262	3200.0754	3211.3862	3210.8816	1647.0169
67	3088.1373	1666.7617	3075.5385	3089.527	3204.696	3215.3246	3215.3607	1666.1942
68	3113.0547	3022.5272	3119.6455	3117.7361	3205.425	3222.4628	3222.0158	3022.932
69	3125.0433	3074.4962	3126.8911	3123.7204	3212.7176	3229.6783	3230.9209	3070.9784
70	3150.0066	3090.6949	3158.6173	3157.4156	3215.6701	-	-	3091.5256
71	3164.0778	3127.433	3174.2415	3158.1202	3224.244	-	-	3122.6272
72	3172.2074	3155.6877	3187.8483	3179.0719	3228.6271	-	-	3157.2046
73	3194.0161	3169.9024	3199.1934	3181.2924	-	-	-	3160.4929
74	3199.2374	3177.5648	3200.6097	3199.1266	-	-	-	3161.1686
75	3211.1344	3189.7854	3211.2881	3210.1057	-	-	-	3198.8652
76	3215.0552	3199.284	3214.5536	3215.1098	-	-	-	3202.1399
77	3222.2555	3211.7666	3222.2844	3221.4666	-	-	-	3209.5447
78	3228.037	3214.014	3225.8464	3229.8032	-	-	-	3214.6255
79	-	3215.0932	-	-	-	-	-	3214.7246
80	-	3222.8884	-	-	-	-	-	3220.9765
81	-	3226.8969	-	-	-	-	-	3228.2378

2. The Boltzmann distribution and its integration

The objective of using a selection of thermometer ions and calculating their survival yield is to reconstruct the internal energy distribution of a benzyl pyridinium salt. This distribution can be described by a Boltzmann distribution such as:

$$P(E) = A\mathrm{E}^{s'-1}e^{\frac{-\mathrm{E}}{\mathrm{k_B}T}} \tag{2}$$

Where A is a normalization factor, E is the energy level where the distribution is evaluated, s' corresponds to the effective number of normal vibrational modes (considering temperature effects on the relative excitation of the different normal modes), k_{B} is the Boltzmann constant, and T is the effective temperature of vibration that describes this distribution.
The survival yield as a function of the dissociation energy plot, gives a S-shaped curve which can be fit by the integral of the Boltzmann distribution:

$$F(E) = \int_0^{\mathrm{E}} P(E)dE \tag{3}$$

First, to find the expression that describes the normalization factor A:

$$F(E) = \int_0^{\infty} P(E)dE = \int_0^{\infty} \mathrm{AE}^{s'-1}e^{\frac{-\mathrm{E}}{\mathrm{k_B}T}}\,\mathrm{dE} \;=\; 1 \tag{4}$$

By performing the variable substitution $u = \frac{E}{k_B T}$, $dE = k_B T\, du$

$$\int_0^{\infty} P(E)dE = \int_0^{\infty} \mathrm{A}(k_B T u)^{s'-1}e^{-u}k_B T\, du \;=\; 1 \tag{5}$$

$$\int_0^{\infty} P(E)dE = A(k_B T)^{s'}\int_0^{\infty} u^{s'-1}e^{-u}du \;=\; 1 \tag{6}$$

This integral results in an expression involving the gamma function $\Gamma(s')$ which is a generalization of factorials applicable to positive non-integer values. It is frequently used in statistical mechanics as it simplifies integrals involving powers of variables and exponential terms. The gamma function is given by:

$$\Gamma(n) \;=\; \int_0^{\infty} t^{n-1}\, e^{-t}\, dt \tag{7}$$

Thus,

$$\int_0^{\infty} P(E)dE = A(k_B T)^{s'}\Gamma(s') = 1 \tag{8}$$

$$A = \frac{1}{(k_B T)^{s'}\Gamma(s')} \tag{9}$$

The next step is finding the expression that describes $F(E)$ by substituting (9) in (4):

$$F(E) = \int_0^{\mathrm{E}} \frac{\mathrm{E}^{s'-1}e^{\frac{-\mathrm{E}}{\mathrm{k_B}T}}}{(k_B T)^{s'}\Gamma(s')}\,\mathrm{dE} \tag{10}$$

Adopting the same variable substitution as before ($u = \frac{E}{k_B T}$, $dE = k_B T\, du$):

$$F(E) = \frac{1}{\Gamma(s')}\int_0^{\frac{\mathrm{E}}{\mathrm{k_B}\mathrm{T}}} \mathrm{u}^{s'-1}e^{-\mathrm{u}}\,\mathrm{du} \tag{11}$$

To solve for $F(E)$, the integral of the energy distribution up to a specific energy value (E) must be evaluated. This involves the use of the lower incomplete gamma function, $\gamma(n,x)$.

While the standard gamma function integrates over the entire range from zero to infinity, the lower incomplete gamma function integrates only up to a finite upper limit, here $(\frac{E}{k_B T})$. The lower incomplete gamma function is defined as:

$$\gamma(n,x) = \int_0^x t^{n-1} e^{-t}\, dt \tag{12}$$

In this context, the expression for $F(E)$ is the ratio of the lower incomplete gamma function $\gamma\left(s', \frac{E}{k_B T}\right)$ to the full gamma function $\Gamma(s')$. This describes how the energy is distributed up to the given energy value E, which corresponds to the fragmentation threshold observed experimentally. Finally,

$$F(E) = \frac{\gamma\left(s', \frac{E}{k_B T}\right)}{\Gamma(s')} \tag{13}$$

At high temperatures, the principle of equipartition of energy across all vibrational modes can be applied, meaning each mode contributes equally to the internal energy. However, at lower temperatures, such as in the case of soft ionization methods in mass spectrometry, a correction factor $c(T)$ is introduced to account for the uneven distribution of energy across the vibrational modes. In this context, the effective (i.e. corrected) number of vibrational degrees of freedom is expressed as $s' = c(T)s$, where s represents the original number of vibrational degrees of freedom $(3N-6)$. This correction reflects the fact that not all vibrational modes are equally excited at lower temperatures, adjusting for their effective contribution to the internal energy.

The correction factor $c(T)$ is given by:

$$\mathrm{c(T)} = \frac{1}{\mathrm{s}} \sum_{\mathrm{i=1}}^{\mathrm{s}} \frac{\frac{\theta_\mathrm{i}}{\mathrm{T}}}{e^{\frac{\theta_\mathrm{i}}{\mathrm{T}}} - 1} \tag{14}$$

Thus, $s' = c(T)s$:

$$\mathrm{s'} = \sum_{\mathrm{i=1}}^{\mathrm{s}} \frac{\frac{\theta_\mathrm{i}}{\mathrm{T}}}{e^{\frac{\theta_\mathrm{i}}{\mathrm{T}}} - 1} \tag{15}$$

where θ_i is the vibrational characteristic temperature of normal mode i defined as:

$$\theta_\mathrm{i} = \frac{\mathrm{hc}\tilde{\nu}_\mathrm{i}}{\mathrm{k_B}} \tag{16}$$

where $\tilde{\nu}_i$ is the wave number of each normal mode of the thermometer ion, h is Planck's constant and c is the speed of light in vacuum.

From the average value of the $P(E)$ function, the average internal energy $\overline{E}_{int}$, can be obtained:

$$\overline{E}_{int} = \frac{\int_0^\infty E\,P(E)dE}{\int_0^\infty P(E)dE} \tag{17}$$

By substituting equations (2), (8) and (9) in equation (24):

$$\overline{E}_{int} = \frac{\int_0^\infty \mathrm{E}^{s'} e^{\frac{-\mathrm{E}}{\mathrm{k_B}T}}\,\mathrm{dE}}{(k_B T)^{s'}\Gamma(s')} \tag{18}$$

By performing the variable substitution $u = \frac{E}{k_B T}$, $dE = k_B T\,du$:

$$\overline{E}_{int} = \frac{(k_B T)\int_0^\infty \mathrm{u}^{s'} e^{-\mathrm{u}}\,\mathrm{du}}{\Gamma(s')} \tag{19}$$

$$\overline{E}_{int} = \frac{(k_B T)\Gamma(s'+1)}{\Gamma(s')} \tag{20}$$

The gamma function has a recursive property that can be expressed as:

$$\Gamma(n+1) = n\Gamma(n) \tag{21}$$

Thus, the average internal energy value can be expressed as:

$$\overline{E}_{int} = s' k_B T = c(T) s k_B T \tag{22}$$

This equation is similar to the one proposed by Vékey[2] in his special feature tutorial.

3. Fitting procedure – integral of the P(E) Boltzmann distribution

The experimental survival yield data are plotted as a function of the dissociation energies (obtained from the DFT computations as explained in section 1). It is recommended that more than one mass spectrum is taken per substrate or matrix for reliability.

By substituting equation (15) in equation (13):

$$SY(E_0) = F(E_0) = \frac{\gamma\left(\sum_{\mathrm{i}=1}^{\mathrm{s}} \frac{\frac{\theta_\mathrm{i}}{\mathrm{T}}}{e^{\frac{\theta_\mathrm{i}}{\mathrm{T}}}-1}, \frac{E_0}{k_B T}\right)}{\Gamma\left(\sum_{\mathrm{i}=1}^{\mathrm{s}} \frac{\frac{\theta_\mathrm{i}}{\mathrm{T}}}{e^{\frac{\theta_\mathrm{i}}{\mathrm{T}}}-1}\right)} \tag{23}$$

The data are fitted using equation (23). Finally, only the T parameter is extracted from the fitting. Since each thermometer ion has its own $\tilde{\nu}_i$ values (and θ_i), this fitting needs to be performed one time for each thermometer used. Therefore, the final effective temperature of vibration ($\mathrm{T_{eff}}$) obtained is an average of those fittings. Here, the selected thermometer ions were benzyl pyridinium salts substituted in the para (p), and meta (m) positions, namely: $\mathrm{pCH_3}(t_1)$, $\mathrm{mCH_3}(t_2)$, pCN (t_3) and $\mathrm{pOCH_3}(t_4)$. Thus, $\mathrm{T_{eff}}$ is given by:

$$T_{eff} = \frac{T_{t_1} + T_{t_2} + T_{t_3} + T_{t_4}}{4} \tag{24}$$

The associated average internal energy could be obtained in a similar way by applying equation (22) to each thermometer ion and averaging the obtained values:

$$\overline{E}_{int} = \frac{k_B(c(T_{t_1})s_{t_1}T_{t_1} + c(T_{t_2})s_{t_2}T_{t_2} + c(T_{t_3})s_{t_3}T_{t_3} + c(T_{t_4})s_{t_4}T_{t_4})}{4} \quad (25)$$

4. Alternative fitting procedure – two parameters logistic curve

An alternative fitting procedure commonly applied in the literature[3,4] relies on fitting the experimental survival yield data (as a function of the dissociation energies) using a two parametric logistic curve. The two obtained parameters are $\boldsymbol{k}$ and $\overline{\boldsymbol{E}}_{\boldsymbol{int}}$ (the average internal energy), such as:

$$\mathbf{SY}\ (\boldsymbol{E_0}) = \frac{\mathbf{1}}{\mathbf{1} + \boldsymbol{e}^{-\mathbf{k}(\mathbf{E_0} - \overline{\mathbf{E}}_{\mathbf{int}})}} \quad (26)$$

The obtained $\overline{\boldsymbol{E}}_{\boldsymbol{int}}$ can then be then inserted in equation (22) and one $\boldsymbol{T}$ value can be obtained for each thermometer ion. It follows that the final effective temperature of vibration ($\mathbf{T_{eff}}$) is obtained by averaging those values such as in equation (24).

Even if this procedure seems more straightforward at a first glance, a few considerations are due:

- The logistic curve is not obtained from the integral of the Boltzmann distribution, therefore no reliable conclusions should be drawn from the width or shape of its derivative
- The obtained values for $\overline{\boldsymbol{E}}_{\boldsymbol{int}}$ and $\mathbf{T_{eff}}$ are indeed similar for both procedures since they only rely on the average value of the distribution that is very similar for the $\boldsymbol{P}(\boldsymbol{E})$ function and the derivative of the logistic function.

Results obtained by applying the fitting procedures proposed in section 4 and 5 can be found in section 6 for comparison.

5. Error propagation throughout different fitting and calculation steps

a. Fitting procedure – integral of the P(E) Boltzmann distribution

Using an in-house python script that relies on a curve fit procedure from the SciPy library, one can have an estimation of the covariance matrix and, thus, the variance of the estimated parameters.

Only one parameter is obtained from the fitting procedure proposed in section 3. Thus, the variance of the temperature σ_{T}^2 is the only value in the covariance matrix.

From the propagation of uncertainties formula (i.e. error propagation or Taylor expansion method), the uncertainty σ_f in f is given by:

$$\boldsymbol{\sigma_f^2} = \sum_{\boldsymbol{i}} \left(\frac{\partial \boldsymbol{f}}{\partial \boldsymbol{\mu_i}}\right)^{\mathbf{2}} \boldsymbol{\sigma_{\mu_i}^2} + \sum_{\boldsymbol{i \neq j}} \frac{\partial \boldsymbol{f}}{\partial \boldsymbol{\mu_i}} \frac{\partial \boldsymbol{f}}{\partial \boldsymbol{\mu_j}} \boldsymbol{cov}(\boldsymbol{\mu_i}, \boldsymbol{\mu_j}) \quad (27)$$

Where $\mu = (\mu_1, \mu_2, \ldots, \mu_n)$ are the parameters of the model, σ_{μ_i} is the individual uncertainty in each parameter and $cov(\mu_i, \mu_j)$ the covariance between parameters.

By applying this formula to equation (22), one can estimate the variance of the average internal energy $\sigma_{\overline{E}_{int}}^2$:

$$\boldsymbol{\sigma^2_{\overline{E}_{int}}} = \left(\frac{\partial \overline{\boldsymbol{E}}_{\boldsymbol{int}}}{\partial \boldsymbol{T}}\right)^{\boldsymbol{2}} \boldsymbol{\sigma^2_T} \tag{28}$$

$$\boldsymbol{\sigma^2_{\overline{E}_{int}}} = \left[\boldsymbol{sk_B}\left(\boldsymbol{T}\,\frac{\boldsymbol{dc(T)}}{\boldsymbol{dT}} + \boldsymbol{c(T)}\right)\right]^{\boldsymbol{2}} \boldsymbol{\sigma^2_T} \tag{29}$$

By taking the derivative in T from equation (14) and substituting in equation (29) , it follows that:

$$\sigma^2_{\overline{E}_{int}} = \left[k_B \sum_{i=1}^{s} \left(\frac{\frac{\theta_i}{T}\left(\frac{\theta_i}{T} e^{\frac{\theta_i}{T}} - \left(e^{\frac{\theta_i}{T}} - 1\right)\right)}{\left(e^{\frac{\theta_i}{T}} - 1\right)^2} + \frac{\frac{\theta_i}{T}}{e^{\frac{\theta_i}{T}} - 1} \right) \right]^2 \sigma^2_T \tag{30}$$

Equation (30) can be simplified to:

$$\boldsymbol{\sigma^2_{\overline{E}_{int}}} = \left[\boldsymbol{k_B} \sum_{\boldsymbol{i=1}}^{\boldsymbol{s}} \left(\frac{\left(\frac{\boldsymbol{\theta_i}}{\boldsymbol{T}}\right)^{\boldsymbol{2}} \boldsymbol{e^{\frac{\theta_i}{T}}}}{\left(\boldsymbol{e^{\frac{\theta_i}{T}}} - \boldsymbol{1}\right)^{\boldsymbol{2}}} \right) \right]^{\boldsymbol{2}} \boldsymbol{\sigma^2_T} \tag{31}$$

Since the values for T and $\overline{E}_{int}$ are averaged across all thermometer ions, it follows that the final variances in T_{eff} and $\overline{E}_{int}$ are given by:

$$\boldsymbol{\sigma^2_T} = \frac{\sum_{\boldsymbol{j=1}}^{\boldsymbol{m}} \boldsymbol{\sigma^2_{T_{t_j}}}}{\boldsymbol{m^2}} \tag{32}$$

$$\boldsymbol{\sigma^2_{\overline{E}_{int}}} = \frac{\sum_{\boldsymbol{j=1}}^{\boldsymbol{m}} \boldsymbol{\sigma^2_{\overline{E}_{int_{t_j}}}}}{\boldsymbol{m^2}} \tag{33}$$

Where t_j represents each thermometer ion used an m is the total number of thermometer ions (here $m = 4$).

b. Alternative fitting procedure – two parameters logistic curve

By fitting the data as proposed in section 4, the variance of the average internal energy $\sigma^2_{\overline{E}_{int}}$ can be obtained from the covariance matrix:

$$C = \begin{bmatrix} \sigma^2_k & cov(\mathrm{k},\overline{\mathrm{E}}_{\mathrm{int}}) \\ cov(\mathrm{k},\overline{\mathrm{E}}_{\mathrm{int}}) & \sigma^2_{\overline{\mathrm{E}}_{\mathrm{int}}} \end{bmatrix} \tag{34}$$

By applying the same principle of equation (27):

$$\boldsymbol{\sigma^2_T} = \left(\frac{\partial \mathbf{T}}{\partial \overline{\boldsymbol{E}}_{\boldsymbol{int}}}\right)^{\boldsymbol{2}} \boldsymbol{\sigma^2_{\overline{\mathrm{E}}_{\mathrm{int}}}} \tag{35}$$

From the relation derived in equation (31):

$$\sigma_T^2 = \frac{\sigma^2_{\overline{\mathrm{E}}_{\mathrm{int}}}}{\left[k_B \sum_{i=1}^{s} \left(\frac{\left(\frac{\theta_i}{T}\right)^2 e^{\frac{\theta_i}{T}}}{\left(e^{\frac{\theta_i}{T}} - 1\right)^2} \right) \right]^2} \tag{36}$$

The final variances in $\mathrm{T}_{\mathrm{eff}}$ can be obtained applying the procedure of equation (32).

6. Results comparison

Figure 1(a) presents the fitted survival yield as a function of dissociation energies, with corresponding error bars for selected substrates. The plot includes both fitting procedures for comparison: the solid line represents the fit using the integral of the $P(E)$ distribution, while the dotted line corresponds to the fit applying a two-parameter logistic curve. The inclusion of error bars for each data point provides a visual representation of the uncertainty in the measurements, offering insights into the precision of the experimental data and the reliability of the fits.

Figure 1(b) displays the probability density function $P(E)$ (i.e. internal energy distributions) for different substrates, using both the $P(E)$ Boltzmann distribution (solid lines) and the two-parameter logistic curve (dotted lines).

The comparison between these two methods reveals that, while both approaches yield similar trends, the $P(E)$ Boltzmann distribution method is more effective at representing sharp transitions in the internal energy distribution. The logistic curve, while capable of fitting the overall shape, tends to overestimate the tails and may not accurately depict the nuances of the peak widths for substrates. This observation underlines the recommendation to use the $P(E)$ Boltzmann distribution when analysing the precise shape and width of the internal energy distribution, as it provides a more accurate representation of the distribution's physical characteristics.Figure *1* - (a) Fitted survival yield as a function of dissociation energies for various substrates, with corresponding data points indicated by markers. The solid lines represent fits using the $\mathrm{P(E)}$ Boltzmann distribution, while the dotted lines indicate fits from a two-parameter logistic model. (b) Probability density function $\mathrm{P(E)}$ of internal energy distributions for the same substrates, illustrating the differences in energy distribution, with solid and dotted lines corresponding to those in panel (a). The coloured legends correspond to the substrates analysed, providing a visual comparison of the fitting methods.

Table ***3*** presents the fitting results obtained by applying the two methods discussed in sections 3 and 4. The effective temperature and average internal energy values differ by less than 1%, underscoring the robustness of both approaches. However, as previously mentioned, when analysing the shape and width of the Boltzmann distribution, it is recommended to use the integral of the P(E) Boltzmann distribution.

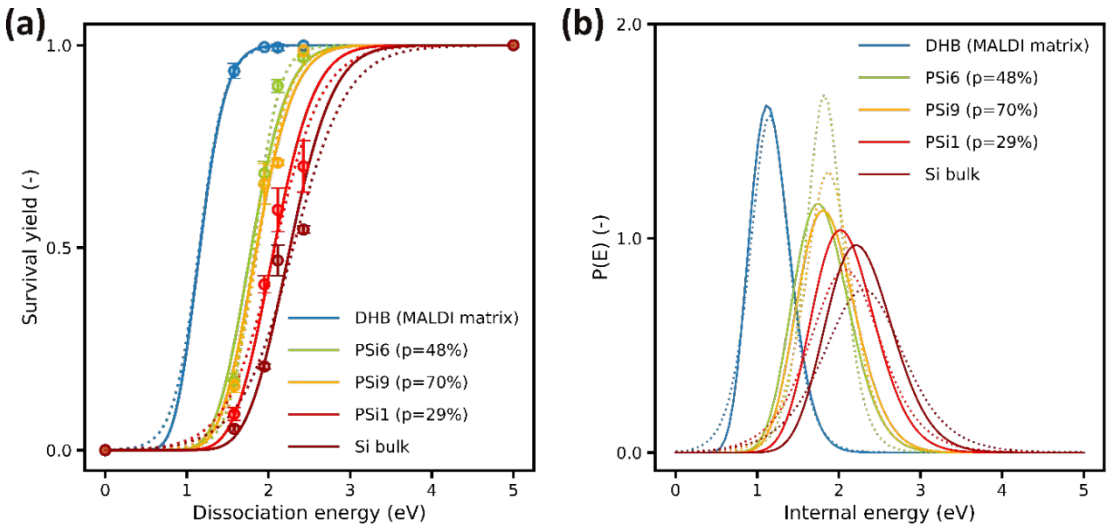

Figure 1 - (a) Fitted survival yield as a function of dissociation energies for various substrates, with corresponding data points indicated by markers. The solid lines represent fits using the $P(E)$ Boltzmann distribution, while the dotted lines indicate fits from a two-parameter logistic model. (b) Probability density function $P(E)$ of internal energy distributions for the same substrates, illustrating the differences in energy distribution, with solid and dotted lines corresponding to those in panel (a). The coloured legends correspond to the substrates analysed, providing a visual comparison of the fitting methods.

Table 3 - Fitting parameters for survival yield and internal energy distributions of various substrates using the integral of the $P(E)$ Boltzmann distribution and the two-parameter logistic curve

			Fitting procedure											
			integral of the P(E) Boltzmann distribution						2-parameters logistic curve					
Substrate	Parent	s	c(T)	T	σ_T	R^2	$\bar{E}_{int}$	$\sigma_{\bar{E}_{int}}$	$\bar{E}_{int}$	$\sigma_{\bar{E}_{int}}$	R^2	c(T)	T	σ_T
PSi1 (p=29%)	mCH3	78	0.369	844.056	5.128	0.905	2.091	0.012	2.079	0.026	0.915	0.368	841.354	5.820
	pCH3	78	0.369	843.826	5.129	0.905	2.091	0.012				0.368	841.126	5.821
	pCN	72	0.392	859.475	5.320	0.907	2.091	0.012				0.391	856.517	6.072
	pOCH3	81	0.366	817.527	5.026	0.901	2.090	0.012				0.365	815.117	5.645
			0.374	**841.221**	**2.576**		**2.091**	**0.006**	**2.079**	**0.026**		**0.373**	**838.528**	**2.921**
PSi2 (p=31%)	mCH3	78	0.358	815.900	2.147	0.878	1.965	0.005	1.946	0.011	0.864	0.357	811.555	2.466
	pCH3	78	0.358	815.668	2.147	0.878	1.965	0.005				0.357	811.325	2.466
	pCN	72	0.382	830.080	2.243	0.879	1.966	0.005				0.380	825.448	2.570
	pOCH3	81	0.356	790.259	2.074	0.877	1.964	0.005				0.355	786.216	2.392
			0.364	**812.977**	**1.077**		**1.965**	**0.002**	**1.946**	**0.011**		**0.362**	**808.636**	**1.237**
PSi3 (p=34%)	mCH3	78	0.352	799.747	1.490	0.891	1.894	0.003	1.877	0.007	0.883	0.351	795.880	1.602
	pCH3	78	0.352	799.515	1.490	0.891	1.894	0.003				0.351	795.648	1.602
	pCN	72	0.375	813.169	1.561	0.891	1.894	0.003				0.374	809.119	1.668
	pOCH3	81	0.350	774.721	1.430	0.891	1.894	0.003				0.349	771.011	1.554
			0.358	**796.788**	**0.747**		**1.894**	**0.002**	**1.877**	**0.007**		**0.356**	**792.914**	**0.804**
PSi4 (p=46%)	mCH3	78	0.346	782.088	1.738	0.872	1.818	0.004	1.807	0.007	0.883	0.345	779.694	1.637
	pCH3	78	0.346	781.855	1.737	0.872	1.818	0.004				0.345	779.460	1.637
	pCN	72	0.369	794.739	1.824	0.870	1.817	0.004				0.368	792.269	1.704
	pOCH3	81	0.344	757.655	1.657	0.874	1.818	0.004				0.343	755.309	1.588
			0.351	**779.084**	**0.870**		**1.818**	**0.002**	**1.807**	**0.007**		**0.350**	**776.683**	**0.821**
PSi5 (p=45%)	mCH3	78	0.346	782.767	4.530	0.954	1.820	0.010	1.823	0.017	0.967	0.346	783.246	3.984
	pCH3	78	0.346	782.536	4.529	0.954	1.820	0.010				0.346	783.013	3.984
	pCN	72	0.369	795.369	4.789	0.953	1.820	0.010				0.369	795.966	4.146
	pOCH3	81	0.344	758.460	4.265	0.956	1.821	0.010				0.344	758.755	3.865
			0.351	**779.783**	**2.266**		**1.821**	**0.005**	**1.823**	**0.017**		**0.351**	**780.245**	**1.998**
PSi6 (p=48%)	mCH3	78	0.345	780.784	4.914	0.954	1.812	0.011	1.823	0.007	0.994	0.346	783.308	1.669
	pCH3	78	0.345	780.552	4.913	0.954	1.812	0.011				0.346	783.075	1.669
	pCN	72	0.368	793.314	5.241	0.953	1.812	0.011				0.369	796.030	1.737
	pOCH3	81	0.343	756.504	4.537	0.958	1.812	0.010				0.344	758.815	1.619

			0.350	**777.788**	**2.454**		**1.812**	**0.005**	**1.823**	**0.007**		**0.351**	**780.307**	**0.837**
PSi7 (p=49%)	mCH3	78	0.344	777.612	5.080	0.903	1.798	0.011	1.816	0.017	0.934	0.346	781.772	4.031
	pCH3	78	0.344	777.380	5.079	0.903	1.798	0.011				0.346	781.539	4.031
	pCN	72	0.367	789.970	5.354	0.901	1.798	0.012				0.368	794.431	4.195
	pOCH3	81	0.342	753.510	4.806	0.906	1.799	0.011				0.344	757.325	3.911
			0.349	**774.618**	**2.542**		**1.798**	**0.006**	**1.816**	**0.017**		**0.351**	**778.767**	**2.022**
PSi8 (p=57%)	mCH3	78	0.347	785.788	2.073	0.837	1.833	0.005	1.831	0.008	0.862	0.347	785.252	1.919
	pCH3	78	0.347	785.556	2.072	0.837	1.834	0.005				0.347	785.019	1.919
	pCN	72	0.370	798.549	2.176	0.836	1.833	0.005				0.370	798.054	1.997
	pOCH3	81	0.345	761.314	1.976	0.840	1.834	0.005				0.345	760.701	1.861
			0.352	**782.802**	**1.038**		**1.834**	**0.002**	**1.831**	**0.008**		**0.352**	**782.256**	**0.962**
PSi9 (p=70%)	mCH3	78	0.351	795.781	4.113	0.963	1.877	0.009	1.871	0.018	0.966	0.350	794.314	4.072
	pCH3	78	0.351	795.550	4.112	0.963	1.877	0.009				0.350	794.082	4.072
	pCN	72	0.374	808.960	4.355	0.963	1.877	0.010				0.373	807.488	4.240
	pOCH3	81	0.349	771.006	3.869	0.965	1.877	0.009				0.348	769.492	3.950
			0.356	**792.824**	**2.058**		**1.877**	**0.005**	**1.871**	**0.018**		**0.356**	**791.344**	**2.042**
CHCA (MALDI matrix)	mCH3	78	0.337	759.447	6.713	0.913	1.721	0.014	1.724	0.014	0.976	0.337	760.208	3.291
	pCH3	78	0.337	759.214	6.712	0.913	1.721	0.014				0.337	759.972	3.292
	pCN	72	0.360	771.084	7.093	0.911	1.720	0.015				0.360	771.999	3.422
	pOCH3	81	0.335	735.867	6.296	0.917	1.722	0.014				0.335	736.403	3.193
			0.342	**756.403**	**3.355**		**1.721**	**0.007**	**1.724**	**0.014**		**0.343**	**757.145**	**1.650**
DHB (MALDI matrix)	mCH3	78	0.281	622.977	2.417	0.892	1.176	0.004	1.153	0.120	0.895	0.278	616.736	32.598
	pCH3	78	0.281	622.741	2.417	0.892	1.176	0.004				0.278	616.481	32.604
	pCN	72	0.301	629.259	2.502	0.892	1.174	0.004				0.298	623.324	33.653
	pOCH3	81	0.280	604.587	2.320	0.892	1.181	0.004				0.277	597.109	31.673
			0.286	**619.891**	**1.207**		**1.177**	**0.002**	**1.153**	**0.120**		**0.283**	**613.413**	**16.320**
Bulk silicon (Si)	mCH3	78	0.384	886.963	6.185	0.838	2.287	0.015	2.303	0.037	0.874	0.385	890.472	7.880
	pCH3	78	0.384	886.735	6.186	0.838	2.287	0.015				0.385	890.247	7.881
	pCN	72	0.408	904.452	6.438	0.842	2.288	0.015				0.409	907.803	8.235
	pOCH3	81	0.381	858.889	6.042	0.832	2.285	0.015				0.382	862.745	7.640
			0.389	**884.260**	**3.107**		**2.287**	**0.008**	**2.303**	**0.037**		**0.390**	**887.817**	**3.956**

7. Porous silicon electrochemical etching conditions

Boron-doped silicon wafers (<100> crystalline orienta-tion, 10-20 mΩ.cm) were electrochemically etched in a 3:3:4 HF(49%): isopropyl alcohol:H2O electrolyte, and rinsed in isopropyl alcohol (IPA). To stabilize the surfaces, a 1 hour oxidation at 350°C under air was performed. Current densities (20 to 100 mA/cm2) and porosification times (16 to 50 seconds) were tuned, with the aid of a Keithley 2460 SourceMeter (Keithley Instruments) to yield the largest possible range of porosities and layer thicknesses of approximately 1 µm. The porosity evolution with current density is consistent with values previously reported in the literature[5].

Table 4 –Porosity before and after oxidation (from spectroscopic liquid infiltration), thickness (from scanning electron microscopy measurements), and electrochemical etching parameters (current density and etching time) for the fabricated porous silicon surfaces.

Porous silicon surface	Freshly-etched sample porosity (%)	Oxidized sample porosity (%)	Thickness (µm)	Current density (mA/cm2)	Etching time (s)
PSi1	26.7 ± 1.6	29.0 ± 2.1	0.870	20	50.00
PSi2	39.5 ± 0.9	31.3 ± 0.7	1.091	35	42.52
PSi3	42.5 ± 0.3	34.0 ± 2.9	1.226	45	33.09
PSi4	51.6 ± 3.5	44.8 ± 3.0	1.222	85	20.53

PSi5	52.1 ± 0.8	45.6 ± 3.1	1.156	80	21.55
PSi6	46.6 ± 2.3	47.7 ± 2.1	0.715	50	25.00
PSi7	52.6 ± 1.1	49.0 ± 0.4	1.029	75	25.00
PSi8	59.2 ± 2.3	56.9 ± 1.6	1.128	90	19.60
PSi9	70.5 ± 2.1	70.3 ± 2.0	0.782	100	16.00

REFERENCES

(1) Rahrt, R.; Auth, T.; Demireva, M.; Armentrout, P. B.; Koszinowski, K. Benzhydrylpyridinium Ions: A New Class of Thermometer Ions for the Characterization of Electrospray-Ionization Mass Spectrometers. *Anal. Chem.* **2019**, *91* (18), 11703–11711. https://doi.org/10.1021/acs.analchem.9b02257.

(2) Vékey, K. Internal Energy Effects in Mass Spectrometry. *J. Mass Spectrom.* **1996**, *31* (5), 445–463. https://doi.org/10.1002/(SICI)1096-9888(199605)31:5<445::AID-JMS354>3.0.CO;2-G.

(3) Luo, G.; Chen, Y.; Daniels, H.; Dubrow, R.; Vertes, A. Internal Energy Transfer in Laser Desorption/Ionization from Silicon Nanowires. *J. Phys. Chem. B* **2006**, *110* (27), 13381–13386. https://doi.org/10.1021/jp0609582.

(4) Carpenter, J. E.; McNary, C. P.; Furin, A.; Sweeney, A. F.; Armentrout, P. B. How Hot Are Your Ions Really? A Threshold Collision-Induced Dissociation Study of Substituted Benzylpyridinium "Thermometer" Ions. *J. Am. Soc. Mass Spectrom.* **2017**, *28* (9), 1876–1888. https://doi.org/10.1007/s13361-017-1693-0.

(5) Lehmann, V. *Electrochemistry of Silicon: Instrumentation, Science, Materials and Applications*, 1st ed.; Wiley, 2002. https://doi.org/10.1002/3527600272.